VOL. 15, NO. 12, JUNE 2020 ISSN 1819-6608
ARPN Journal of Engineering and Applied Sciences

www.arpnjournals.com

LARGE PARAMETER SPECTRAL PERTURBATION APPROACH FOR DOUBLE DIFFUSIVE NATURAL CONVECTION FLOW THROUGH A MAGNETIZED VERTICAL PERMEABLE PLATE

T. M. Agbaje and P. G. L. Leach
Institute of Systems Science, Durban University of Technology, Durban, South Africa
E-Mail: titilayoagbaje@gmail.com

ABSTRACT

In this paper, a new approach for solving the system of coupled nonlinear partial differential equations that model fluid flow problems. The method, called the large parameter spectral perturbation method (LSPM) uses series expansion about a large parameter to decompose the system of partial differential equations (PDEs) into a sequence of ordinary differential equations (ODEs). The sequence of ODEs is then solved using the Chebyshev spectral collocation method. The LSPM is tested on a coupled three-equation system that models the problem of natural convection heat transfer flow through a magnetized vertical permeable plate for liquid metals. The accuracy of the LSPM is tested against the multi-domain bivariate spectral quasilinearisation method (MD-BSQLM) which is an approach that uses the quasilinearisation technique to linearise the nonlinear PDEs first and thereafter using the Chebyshev spectral collocation method to solve the governing equations on a sequence of smaller non-overlapping sub-intervals. The approximate numerical results indicate that the LSPM is an accurate and computationally efficient method for solving coupled nonlinear systems of PDEs defined over a large parameter interval. The numerical results obtained are presented graphically to show the effect of different parameters on the temperature, velocity profiles and transverse component field for different values of some of the parameters. Approximate numerical results for local skin friction, current density, and rate of heat transfer are presented in tabular forms. Residual error graphs are presented in order to further show the accuracy of the LSPM. We remark also that this paper aims at correcting the errors introduced by wrong transformations evident in the system of equations which have been chosen from literature for the numerical experiment.

Keywords: series solution approach; multi-domain bivariate spectral quasilinearisation method; magnetic field; error analysis; vertical permeable plate.

1. INTRODUCTION

Boundary layer flows are most important problems of fluid mechanics with both so many applications theoretically and practically. These classes of problems are modelled by nonlinear partial differential equations (PDEs). Boundary layer flow equations occur frequently in engineering, physics and have substantial applications in the extrusion of plastic sheet, food processing, cooling process of metallic plates, and many other fields. Most physical problems which model systems in nature leads to nonlinear partial differential equations (PDEs). Examples of such physical problems include heat transfer, biological systems, engineering and fluid flow. To have a better understanding of the behaviour of these problems, it is crucial to find solutions of these PDEs. The prominent challenge is the non-existence of analytic solutions to most nonlinear PDEs modelling real life problems because the PDEs are highly nonlinear and complex to solve exactly even with the use of computing software.

To overcome this challenge, a number of numerical and analytical methods have been developed by researchers to approximate the solutions to these nonlinear boundary layer PDEs. Examples of analytical methods that have used by researchers to solve systems of nonlinear boundary layer partial differential equations include perturbation series approach used by Ashraf *et al.* [1], differential transform method used by Abd-Elaziz and Sameh [2], and homotopy analysis method used by Liao [3] amongst others. The finite difference method employed by Kumari and Nath [4] is an example of such numerical methods commonly used by researchers to solve such nonlinear partial differential equations. These methods have their own advantages and disadvantages. For instance, a limiting factor of the approximate analytical method is that it may be difficult to obtain closed form solution in some cases for a nonlinear system involving many coupled equations. There are limits to how the approximate analytical approaches can be applied in nonlinear systems involving many coupled equations. Furthermore, numerical methods may fail to work when the domain is large $\xi > 1$. The finite difference method for example also may require many grid points to achieve an accurate result and, hence, requires a lot of computational time and computer memory.

In an attempt to eliminate some of the numerical methods limitations, recent advances in the developments of numerical methods have focused on Chebyshev spectral collocation based approaches for solving some nonlinear PDEs which require few grid points to give accurate results. Some of the Chebyshev spectral collocation based methods that have been used to solve systems of nonlinear boundary layer partial differential equations include bivariate spectral relaxation method [5], bivariate spectral quasilinearisation method [6], bivariate spectral local linearisation method [7] and bivariate spectral homotopy analysis method [8]. However, there are limits to how these Chebyshev spectral collocation based methods can

be utilized in nonlinear systems of PDEs especially those problems defined over large intervals. There is no guarantee that the resulting approximate numerical solution from these methods mentioned above will be accurate when the nonlinear PDEs are defined over large intervals. This is because the numerical solution may not converge to the required solution even when a large number of grid points is used. To accurately solve a problem over large domains, a fine grid with many collocation points may be required. Using far too many grid points leads to a deterioration of the accuracy of the spectral methods.

The aim of this study is to introduce an alternative approach called the large parameter spectral perturbation method (LSPM) that will be able to handle a wide variety of systems of nonlinear boundary layer PDEs that model fluid mechanics problems that are defined over large intervals. The LSPM blends the asymptotic analysis idea with numerical solution techniques. The method uses the Chebyshev spectral collocation method to gain numerical approximate solution of higher order asymptotic series equations which may be difficult to obtain analytically. The analytical version of the large parameter method has been used by Hossain et al. [9] to solve a non-similar system of nonlinear boundary layer partial equations exactly. In the large parameter method used by the above mentioned authors, the nature of the problems they considered was in such a way that the series solution can be obtained exactly.

In this present study, we examine that the sequence of ordinary differential equations (ODEs) which are given by the series expansion has variable coefficients and may be complex to solve exactly as the order of the approximation increases, hence, the introduction of the Chebyshev spectral collocation method to solve the higher order perturbation equations numerically. We demonstrate that the range of validity of the spectral perturbation method (SPM) [10] can be extended by doing the series expansion about a large parameter. The SPM is a series expansion based method that depends on the existence of a small perturbation parameter in an equation. The SPM combines the idea of the standard perturbation series techniques and the Chebyshev spectral collocation method. In the SPM, we regard ξ as a small perturbation parameter and then search for a perturbation series approximation of the governing equations. The resulting sequence of ODEs generated by the perturbation series approximation is then solved numerically using the Chebyshev spectral collocation method and this method was used in this study because spectral methods are well documented to be a good numerical tool for ordinary differential equations with variable coefficients. Furthermore, in this study, simple decoupled linear systems formulas for generating the solutions in the form of decoupled linear systems were derived.

In order to demonstrate the applicability of the LSPM, we revisit the natural convection heat transfer flow past a magnetized vertical permeable plate for liquid metals that was previously investigated by [1] using the finite difference method, and the perturbation series approach. It is worth mentioning here that the asymptotic series method transformation of equation (2) reported by [1] was erroneous and as a result of that, the transformed F and Φ equations [1] presented were incorrect. In this work, we present the valid transformations and correct equations. The accuracy of the LSPM is validated against results generated using the multi-domain bivariate spectral quasilinearisation method (MD-BSQLM). The MD-BSQLM uses the idea of the quasilinearisation, Chebyshev spectral collocation, and bivariate Lagrange interpolation. In the MD-BSQLM, the governing nonlinear systems of PDEs are linearized using the newton Raphson based quasilinearisation method of Bellman and Kalaba [11] and then integrating the resulting equations in multiple sub-intervals using the Chebyshev spectral collocation method. The Chebyshev spectral collocation method with the Lagrange interpolation polynomials are applied to the linearised nonlinear systems of PDEs independently in both space and time direction. The LSPM also approximates the solution of the problem in fractions of a second and converges faster than the MD-BSQLM. The computational speed of the LSPM can be explained by the fact that, unlike the MD-BSQLM and other numerical methods, the LSPM solves a partial differential equation by applying discretization only in the space direction. Results are presented in tabular and graphical forms. The two methods are compared in terms of easy implementation, accuracy and computational speed. In order to further demonstrate the accuracy of the LSPM, residual error graphs are presented to show the accuracy of the method. The effects of transverse component magnetic field, pertinent parameters on velocity profile and temperature profile are also examined and presented graphically.

2. GOVERNING EQUATIONS

In this section, we reconsider a steady and two-dimensional natural convection flow of an electrically conducting viscous and incompressible fluid past a uniformly heated vertical plate for liquid metals previously investigated by Ashraf et al. [1]. The surface mass flux V_0 is assumed to be uniform. The surface mass flux is negative when the fluid is withdrawn through the surface while when the fluid is blown through the surface, the surface mass flux is positive. In this present study, the case of withdrawal of fluid from the surface shall be considered. The governing equations can be expressed in dimensionless form as [1]:

$$f''' + \frac{3}{4}ff'' - \frac{1}{2}f'^2 + \theta - S\left(\frac{3}{4}\phi\phi'' - \frac{1}{2}\phi'^2\right) + \xi f'' = \frac{1}{4}\xi\begin{bmatrix} f'\frac{\partial f'}{\partial \xi} - f''\frac{\partial f}{\partial \xi} \\ -S\left(\phi'\frac{\partial \phi'}{\partial \xi} - \phi''\frac{\partial \phi}{\partial \xi}\right)\end{bmatrix}, \quad (1)$$

$$\frac{1}{Pm}\phi''' + \frac{3}{4}f\phi'' - \frac{3}{4}f''\phi + \xi\phi'' = \frac{1}{4}\xi\left[f'\frac{\partial \phi'}{\partial \xi} - \phi'\frac{\partial f'}{\partial \xi} + f''\frac{\partial \phi}{\partial \xi} - \phi''\frac{\partial f}{\partial \xi}\right], \quad (2)$$

$$\frac{1}{Pr}\theta'' + \frac{3}{4}f\theta' + \xi\theta' = \frac{1}{4}\xi\left[f'\frac{\partial\theta\prime}{\partial\xi} - \theta'\frac{\partial f}{\partial\xi}\right] \quad (3)$$

subject to

$$f(\xi,0) = f'(\xi,0) = 0, \quad \phi(\xi,0) = 0, \phi'(\xi,0) = 1, \quad \theta(\xi,0) = 1,$$
$$f'(\xi,\infty) = \phi'(\xi,\infty) = \theta(\xi,\infty) = 0. \quad (4)$$

In the above equations prime denotes differentiation with respect to η, and ξ is the transpiration parameter, S is the magnetic force parameter, Pm the magnetic Prandtl number, and Pr the Prandtl number. The non-dimensional skin friction coefficients, rate of heat transfer and current density are given in [1] as;

$$Gr_L^{-3/4}x^{-1/4}C_f = f''(0,\xi), \quad Gr_L^{-3/4}x^{-1/4}J_w = -\phi''(0,\xi), \quad Gr_L^{1/4}x^{1/4}N_u = -\theta'(0,\xi). \quad (5)$$

3. LARGE PARAMTER SPECTRAL PERTURBATION METHOD (LSPM)

In this section, we derive the simplified form to finding the solution to equations (1 - 3) along side with the boundary conditions (4) when the transpiration parameter ξ is large. The order of magnitude of different terms in (1 - 3) shows that the terms with the largest magnitude in (1) are f''' and $\xi f''$, in (2) ϕ''' and $\xi\phi''$, and θ'' and $\xi\theta'$ in (3). Both the terms have to be balanced in the respective equations and the only way to do this is to assume that η to be small and its derivatives are large. Given that $\theta = O(1)$ as $\xi \to \infty$, it is necessary to find appropriate scaling for f and η. On balancing the f''' , θ and $\xi f''$ terms in (1) using the method of dominant balance, it is found that $\eta = O(\xi^{-1})$, $f = O(\xi^{-3})$ and $\phi = O(\xi^{-1})$ as $\xi \to \infty$. Therefore, the following transformations are introduced

$$f = \xi^{-3}F(\bar{\eta}), \bar{\eta} = \xi\eta, \quad \phi = \xi^{-1}\Phi(\bar{\eta}), \quad \theta = \Theta(\bar{\eta}). \quad (6)$$

Substituting these transformations given in (6) into equations (1 - 3), we obtain the following equations:

$$\mathrm{F}''' + \mathrm{F}'' + \Theta - \frac{1}{2}\mathrm{S}\Phi\Phi'' + \frac{1}{2}\mathrm{S}\Phi'^2 = \frac{1}{4}\xi^{-3}\left[\mathrm{F}'\frac{\partial \mathrm{F}\prime}{\partial\xi} - \mathrm{F}''\frac{\partial \mathrm{F}}{\partial\xi}\right] - \frac{1}{4}\xi\mathrm{S}\left[\Phi'\frac{\partial\Phi\prime}{\partial\xi} - \Phi''\frac{\partial\Phi}{\partial\xi}\right], \quad (7)$$

$$\Phi''' + \mathrm{Pm}\Phi'' - \frac{1}{2}\mathrm{Pm}\xi^{-4}\mathrm{F}''\Phi - \frac{1}{2}\mathrm{Pm}\xi^{-4}\mathrm{F}'\Phi' = \frac{1}{4}\mathrm{Pm}\xi^{-3}\left[\mathrm{F}'\frac{\partial\Phi\prime}{\partial\xi} - \Phi'\frac{\partial \mathrm{F}\prime}{\partial\xi} + \mathrm{F}''\frac{\partial\Phi}{\partial\xi} - \Phi''\frac{\partial \mathrm{F}}{\partial\xi}\right], \quad (8)$$

$$\Theta'' + \mathrm{Pr}\Theta' = \frac{1}{4}\mathrm{Pr}\xi^{-3}\left[\mathrm{F}'\frac{\partial\Theta}{\partial\xi} - \Theta'\frac{\partial \mathrm{F}}{\partial\xi}\right]. \quad (9)$$

The corresponding boundary conditions are given by

$$\mathrm{F}(\xi,0) = \mathrm{F}'(\xi,0) = 0, \quad \Phi(\xi,0) = 0, \quad \Phi'(\xi,0) = 1, \quad \Theta(\xi,0) = 1, \quad \mathrm{F}'(\xi,\infty) = \Phi'(\xi,\infty) = \Theta(\xi,\infty) = 0. \quad (10)$$

Since ξ is large, solutions of equations (7 - 9) are obtained using the perturbation method. Hence, we expand the functions $F(\xi,\bar{\eta})$, $\Phi(\xi,\bar{\eta})$ and $\Theta(\xi,\bar{\eta})$ in powers of ξ^{-4} as given below:

$$F(\xi,\bar{\eta}) = \sum_{k=0}^{\infty}\xi^{-4k}F_k(\bar{\eta}), \quad (11)$$

$$\Phi(\xi,\bar{\eta}) = \sum_{k=0}^{\infty}\xi^{-4k}\Phi_k(\bar{\eta}), \quad (12)$$

$$\Theta(\xi,\bar{\eta}) = \sum_{k=0}^{\infty}\xi^{-4k}\Theta_k(\bar{\eta}). \quad (13)$$

It is worth mentioning here that the transformation given in equation (6) for ϕ is the valid transformation for equation (2). This led to equations (7 - 8) and the expansion used in (11 - 13) being different from the ones reported in literature by Ashraf *et al.* [1]. Substituting equations (11 - 13) into equations (7) - (9) and then equating the coefficients of like powers of ξ, we obtain the equations for $k = 0$ as

$$F_0''' + F_0'' + \Theta_0 - \frac{1}{2}S\Phi_0\Phi_0'' + \frac{1}{2}S\Phi_0'^2 = 0, \quad (14)$$

$$\Phi_0''' + Pm\Phi_0'' = 0, \quad (15)$$

$$\Theta_0'' + Pr\Theta_0' = 0, \quad (16)$$

subject to the following boundary conditions

$$\mathrm{F}_0(0) = \mathrm{F}_0'(0) = 0, \quad \Phi_0(0) = 0, \quad \Phi_0'(0) = 1, \quad \Theta_0(0) = 1, \quad \mathrm{F}_0'(\infty) = \Phi_0'(\xi,\infty) = \Theta_0(\infty) = 0. \quad (17)$$

The equations for k ≥ 1 are given as

$$F_k''' + F_k'' + \Theta_k - \frac{1}{2}S\Phi_0\Phi_k'' + \frac{1}{2}S\Phi_0'\Phi_k' - S\Phi_0'k\Phi_k' + S\Phi_0''k\Phi_k = \left[\sum_{n=0}^{k-1}F_{k-1-n}''nF_n - \sum_{n=0}^{k-1}F_{k-1-n}'nF_n'\right] + \mathrm{S}\left[\frac{1}{2}\sum_{\mathrm{n}=0}^{\mathrm{k}-1}\Phi_{\mathrm{k}-\mathrm{n}}\Phi_{\mathrm{n}}'' - \frac{1}{2}\sum_{\mathrm{n}=0}^{\mathrm{k}-1}\Phi_{\mathrm{k}-\mathrm{n}}'\Phi_{\mathrm{n}}' + \sum_{\mathrm{n}=0}^{\mathrm{k}-1}\Phi_{\mathrm{k}-\mathrm{n}}'\mathrm{n}\Phi_{\mathrm{n}}' - \sum_{\mathrm{n}=0}^{\mathrm{k}-1}\Phi_{\mathrm{k}-\mathrm{n}}''\mathrm{n}\Phi_{\mathrm{n}}\right], \quad (18)$$

$$\Phi_{\mathrm{k}}''' + \mathrm{Pm}\Phi_{\mathrm{k}}'' = \frac{1}{2}\mathrm{Pm}\sum_{\mathrm{n}=0}^{\mathrm{k}-1}\mathrm{F}_{\mathrm{k}-1-\mathrm{n}}'^{\Phi_{\mathrm{n}}\prime} + \frac{1}{2}\mathrm{Pm}\sum_{\mathrm{n}=0}^{\mathrm{k}-1}\mathrm{F}_{\mathrm{k}-1-\mathrm{n}}''^{\Phi_{\mathrm{n}}} - \mathrm{Pm}\sum_{\mathrm{n}=0}^{\mathrm{k}-1}\mathrm{F}_{\mathrm{k}-1-\mathrm{n}}'\mathrm{n}\Phi_{\mathrm{n}}' + \mathrm{Pm}\sum_{\mathrm{n}=0}^{\mathrm{k}-1}\Phi_{\mathrm{k}-1-\mathrm{n}}'\mathrm{n}\mathrm{F}_{\mathrm{n}}' - \mathrm{Pm}\sum_{\mathrm{n}=0}^{\mathrm{k}-1}\mathrm{F}_{\mathrm{k}-1-\mathrm{n}}''\mathrm{n}\Phi_{\mathrm{n}} + \mathrm{Pm}\sum_{\mathrm{n}=0}^{\mathrm{k}-1}\Phi_{\mathrm{k}-1-\mathrm{n}}''\mathrm{n}\mathrm{F}_{\mathrm{n}}, \quad (19)$$

$$\Theta_{\mathrm{k}}'' + \mathrm{Pr}\Theta_{\mathrm{k}}' = \mathrm{Pr}\left[\sum_{\mathrm{n}=0}^{\mathrm{k}-1}\Theta_{\mathrm{k}-1-\mathrm{n}}'\mathrm{n}\mathrm{F}_{\mathrm{n}} - \sum_{\mathrm{n}=0}^{\mathrm{k}-1}\mathrm{F}_{\mathrm{k}-1-\mathrm{n}}'\mathrm{n}\Theta_{\mathrm{n}}\right], \quad (20)$$

$$\mathrm{F}_{\mathrm{k}}(0) = 0, \quad \mathrm{F}_{\mathrm{k}}'(0) = 0, \quad \mathrm{F}_{\mathrm{k}}'(\infty) = 0, \quad \Phi_{\mathrm{k}}(0) = 0, \quad \Phi_{\mathrm{k}}'(0) = 0, \quad \Phi_{\mathrm{k}}'(\infty) = 0, \quad \Theta_k(0) = 0, \Theta_k(\infty) = 0. \quad (21)$$

The initial solution at $k = 0$ used to start the LSPM algorithm, is given by equations (14 - 16) subject to the boundary conditions (17). Solving these equations exactly gives

$$F_0(\bar{\eta}) = \frac{e^{Pr\bar{\eta}} - Pre^{-\bar{\eta}}}{(Pr-1)Pr^2} + \frac{S\left(e^{Pm\bar{\eta}} - Pme^{-\bar{\eta}}\right)}{2(Pm-1)Pm^2} + \frac{2Pm^2 + Pr^2 S}{2PmPr^2} \quad (22)$$

$$\Phi_0(\bar{\eta}) = \frac{1 - e^{-Pm\bar{\eta}}}{Pm}, \quad (23)$$

$$\Theta_0(\bar{\eta}) = e^{-Pr\bar{\eta}}. \quad (24)$$

The solution to equations (18 - 20) can be obtained using the Chebyshev spectral collocation method since the left hand side of the higher order perturbation equations (18 - 20) is linear. We remark that in view of equation (18) having variable coefficients, F_k, Φ_k, Θ_k may be complex to solve exactly as the order of the series approximation increases. It is for that reason we employ the Chebyshev spectral collocation method to gain numerical approximate solution of equations (18 -20) and that is why the method is called large parameter spectral perturbation method. For brevity, we remark that the details of the Chebyshev spectral collocation method have been omitted in this work. Further details of how the Chebyshev spectral collocation method can be used to solve related PDEs with fluid mechanics applications can be found in (see for example ([5, 6, 10])). Applying the Chebyshev spectral collocation method on equations (18 - 20) gives

$$\mathrm{A}_{1,\mathrm{k}-1}\mathrm{F}_\mathrm{k} = \mathrm{B}_{1,\mathrm{k}-1}, \quad \mathrm{A}_{2,\mathrm{k}-1}\boldsymbol{\Phi}_\mathrm{k} = \mathrm{B}_{2,\mathrm{k}-1}, \quad \mathrm{A}_{3,\mathrm{k}-1}\boldsymbol{\Theta}_\mathrm{k} = \mathrm{B}_{3,\mathrm{k}-1}, \quad (25)$$

where

$A_{1,k-1}, A_{2,k-1}, A_{3,k-1}, B_{1,k-1}, B_{2,k-1}, \text{and} B_{3,k-1}$ are defined as

$$\mathrm{A}_{1,\mathrm{k}-1} = \mathrm{D}^3 + \mathrm{D}^2 - \mathrm{diag}\left(\frac{1}{2}\mathrm{S}\boldsymbol{\Phi}_0\right)\mathrm{D}^2\boldsymbol{\Phi} + \mathrm{diag}\left(\frac{1}{2}\mathrm{S}(\mathrm{D}\boldsymbol{\Phi}_0)\right)\mathrm{D}\boldsymbol{\Phi}$$

$$-\mathrm{k}\,\mathrm{diag}(\mathrm{S}(\mathrm{D}\boldsymbol{\Phi}_0))\mathrm{D}\boldsymbol{\Phi} + \mathrm{k}\,\mathrm{diag}(\mathrm{S}(\mathrm{D}^2\boldsymbol{\Phi}_0)), \quad (26)$$

$$\mathrm{A}_{2,\mathrm{k}-1} = \mathrm{D}^2 + \mathrm{PmD}, \quad \mathrm{A}_{3,\mathrm{k}-1} = \mathrm{D}^2 + \mathrm{PrD}, \quad (27)$$

$$\mathrm{B}_{1,\mathrm{k}-1} = \mathrm{SumF} - \boldsymbol{\Theta}_\mathrm{k}, \quad \mathrm{B}_{2,\mathrm{k}-1} = \mathrm{Sum}\boldsymbol{\Phi}, \quad \mathrm{B}_{3,\mathrm{k}-1} = \mathrm{Sum}\boldsymbol{\Theta}, \quad (28)$$

where $\mathrm{SumF}, \mathrm{Sum}\boldsymbol{\Phi}$ and $\mathrm{Sum}\boldsymbol{\Theta}$ are defined as;

$$\mathrm{SumF} = \frac{1}{2}\mathrm{S}\sum_{\mathrm{n}=0}^{\mathrm{k}-1}\boldsymbol{\Phi}_{\mathrm{k}-\mathrm{n}}(\mathrm{D}^2\boldsymbol{\Phi}_\mathrm{n}) - \frac{1}{2}\mathrm{S}\sum_{\mathrm{n}=0}^{\mathrm{k}-1}(\mathrm{D}\boldsymbol{\Phi}_{\mathrm{k}-\mathrm{n}})(\mathrm{D}\boldsymbol{\Phi}_\mathrm{n}) - \sum_{\mathrm{n}=0}^{\mathrm{k}-1}(\mathrm{DF}_{\mathrm{k}-1-\mathrm{n}})(\mathrm{nDF}_\mathrm{n})$$
$$+\sum_{\mathrm{n}=0}^{\mathrm{k}-1}(\mathrm{D}^2\mathrm{F}_{\mathrm{k}-1-\mathrm{n}})(\mathrm{nF}_\mathrm{n}) + \mathrm{S}\sum_{\mathrm{n}=0}^{\mathrm{k}-1}(\mathrm{D}\boldsymbol{\Phi}_{\mathrm{k}-\mathrm{n}})(\mathrm{nD}\boldsymbol{\Phi}_\mathrm{n}) - \mathrm{S}\sum_{\mathrm{n}=0}^{\mathrm{k}-1}(\mathrm{D}^2\boldsymbol{\Phi}_{\mathrm{k}-\mathrm{n}})(\mathrm{n}\boldsymbol{\Phi}_\mathrm{n}),$$

$$\mathrm{Sum}\boldsymbol{\Phi} = \frac{1}{2}\mathrm{Pm}\sum_{\mathrm{n}=0}^{\mathrm{k}-1}(\mathrm{DF}_{\mathrm{k}-1-\mathrm{n}})(\mathrm{D}\boldsymbol{\Phi}_\mathrm{n}) + \frac{1}{2}\mathrm{Pm}\sum_{\mathrm{n}=0}^{\mathrm{k}-1}(\mathrm{D}^2\mathrm{F}_{\mathrm{k}-1-\mathrm{n}})\boldsymbol{\Phi}_\mathrm{n} - \mathrm{Pm}\sum_{\mathrm{n}=0}^{\mathrm{k}-1}(\mathrm{DF}_{\mathrm{k}-1-\mathrm{n}})(\mathrm{nD}\boldsymbol{\Phi}_\mathrm{n})$$
$$+\mathrm{Pm}\sum_{\mathrm{n}=0}^{\mathrm{k}-1}(\mathrm{D}\boldsymbol{\Phi}_{\mathrm{k}-1-\mathrm{n}})(\mathrm{nDF}_\mathrm{n}) - \mathrm{Pm}\sum_{\mathrm{n}=0}^{\mathrm{k}-1}(\mathrm{D}^2\mathrm{F}_{\mathrm{k}-1-\mathrm{n}})(\mathrm{n}\boldsymbol{\Phi}_\mathrm{n}) + \mathrm{Pm}\sum_{\mathrm{n}=0}^{\mathrm{k}-1}(\mathrm{D}^2\boldsymbol{\Phi}_{\mathrm{k}-1-\mathrm{n}})(\mathrm{nF}_\mathrm{n}),$$

$$\mathrm{Sum}\boldsymbol{\Theta} = \mathrm{Pr}\sum_{\mathrm{n}=0}^{\mathrm{k}-1}(\mathrm{D}\boldsymbol{\Theta}_{\mathrm{k}-1-\mathrm{n}})(\mathrm{nF}_\mathrm{n}) - \mathrm{Pr}\sum_{\mathrm{i}=0}^{\mathrm{k}-1}(\mathrm{DF}_{\mathrm{k}-1-\mathrm{n}})(\mathrm{n}\boldsymbol{\Theta}_\mathrm{n}),$$

Thus, starting from a known F_0, Θ_0, Φ_0, the solutions F_k, Φ_k, Θ_k, for $k \geq 1$ can be obtained from equation (25) as

$$F_k = A_{1,k-1}^{-1}B_{1,k-1}, \boldsymbol{\Phi}_k = A_{2,k-1}^{-1}B_{2,k-1}, \boldsymbol{\Theta}_k = A_{3,k-1}^{-1}B_{3,k-1}. \quad (29)$$

4. MULTI-DOMAIN BIVARIATE SPECTRAL QUASILINEARISATION METHOD (MD-BSQLM)

In this section, we briefly describe how the multi-domain spectral quasilinearisation (MD-BSQLM) method of solution is been used to solve equations (1 - 3). The MD-BSQLM is based on using the quasiliearisation method proposed by Bellman and Kalaba [11] to linearise the governing equation and use the Chebyshev spectral collocation method to solve the linearised equations in a sequence of sub-intervals. The multi-domain or multistage or piece-wise approach has been previously used to solve IVPs modelled by chaotic, hyperchaotic and noncahotic systems (see Nik and Rebelo [12], Effati *et al.* [13] and Goh *et al.* [14]). The multi-domain is applied only in the ξ direction. To implement the multi-domain, we first linearise equations (1 - 3) using the quasilinearisation (QLM). The quasiliearisation method uses the Newton Raphson based qualinearisation method of Bellman and Kalaba [11] to linearise the governing equations and solves the resulting system of linearised equations using the Chebyshev spectral collocation method. Applying the QLM on (1 - 3) gives

$$a_{0,r}(\eta,\xi){f_{r+1}}''' + a_{1,r}(\eta,\xi){f_{r+1}}'' + a_{2,r}(\eta,\xi){f_{r+1}}' + a_{3,r}(\eta,\xi)f_{r+1} + a_{4,r}(\eta,\xi)\frac{\partial {f'}_{r+1}}{\partial\xi} + a_{5,r}(\eta,\xi)\frac{\partial f_{r+1}}{\partial\xi} + a_{6,r}(\eta,\xi){\phi_{r+1}}'' + a_{7,r}(\eta,\xi){\phi_{r+1}}' + a_{8,r}(\eta,\xi)\phi_{r+1} + a_{9,r}(\eta,\xi)\frac{\partial {\phi'}_{r+1}}{\partial\xi} + a_{10,r}(\eta,\xi)\frac{\partial\phi_{r+1}}{\partial\xi} + a_{11,r}(\eta,\xi)\theta_{r+1} = R_{1,r}(\eta,\xi), \quad (30)$$

$$b_{0,r}(\eta,\xi){\phi_{r+1}}''' + b_{1,r}(\eta,\xi){\phi_{r+1}}'' + b_{2,r}(\eta,\xi){\phi_{r+1}}' + b_{3,r}(\eta,\xi)\phi_{r+1} + b_{4,r}(\eta,\xi)\frac{\partial {\phi'}_{r+1}}{\partial\xi} + b_{5,r}(\eta,\xi)\frac{\partial\phi_{r+1}}{\partial\xi} + b_{6,r}(\eta,\xi){f_{r+1}}'' + b_{7,r}(\eta,\xi){f_{r+1}}' + b_{8,r}(\eta,\xi)f_{r+1} + +b_{9,r}(\eta,\xi)\frac{\partial {f_{r+1}}'}{\partial\xi} + b_{10,r}(\eta,\xi)\frac{\partial f_{r+1}}{\partial\xi} = R_{2,r}(\eta,\xi), \quad (31)$$

$$c_{0,r}(\eta,\xi)\theta_{r+1}'' + c_{1,r}(\eta,\xi)\theta_{r+1}' + c_{2,r}(\eta,\xi)\theta_{r+1} + c_{3,r}(\eta,\xi)\frac{\partial\theta_{r+1}}{\partial\xi} + c_{4,r}(\eta,\xi){f'}_{r+1} + c_{5,r}(\eta,\xi)f_{r+1} + c_{6,r}(\eta,\xi)\frac{\partial f_{r+1}}{\partial\xi} = R_{3,r}(\eta,\xi), \quad (32)$$

subject to the boundary conditions

$$f_{r+1}(0,\xi)=0,\quad {f_{r+1}}'(0,\xi)=0,\quad {f'}_{r+1}(\infty,\xi)=0,\quad \phi_{r+1}(0,\xi)=0,\quad {\phi_{r+1}}'(0,\xi)=1,\quad {\phi_{r+1}}'(\infty,\xi)=0,\quad \theta_{r+1}(0,\xi)=1,\quad \theta_{r+1}(\infty,\xi)=0, \quad (33)$$

where

$$a_{0,r}=1,\quad a_{1,r}=\frac{3}{4}fr+\xi+\frac{1}{4}\xi\frac{\partial f_r}{\partial\xi},\quad a_{2,r}=-{f_r}'-\frac{1}{4}\xi\frac{\partial {f_r}'}{\partial\xi}\,a_{3,r}=\frac{3}{4}{f_r}'',\quad a_{4,r}=-\frac{1}{4}\xi{f_r}',$$

$$a_{5,r}=\frac{1}{4}\xi{f_r}'',\quad a_{6,r}=-\frac{3}{4}S{\phi'}_r-\frac{1}{4}\xi S\frac{\partial\phi_r}{\partial\xi},\quad a_{7,r}=S{\phi'}_r+\frac{1}{4}\xi S\frac{\partial{\phi'}_r}{\partial\xi},\quad a_{8,r}=-\frac{3}{4}S{\phi''}_r,$$

$$a_{9,r}=\frac{1}{4}\xi S{\phi'}_r,\quad a_{10,r}=-\frac{1}{4}\xi S{\phi'}_r,\quad a_{11,r}=1,$$

$$b_{0,r}=1,\quad b_{1,r}=\frac{3}{4}Pmf_r+Pm\xi+\frac{1}{4}Pm\xi\frac{\partial f_r}{\partial\xi},\quad b_{2,r}=\frac{1}{4}Pm\xi\frac{\partial {f_r}'}{\partial\xi},\quad b_{3,r}=-\frac{3}{4}Pm{f_r}'',$$

$$b_{4,r}=-\frac{1}{4}Pm\xi{f_r}',\quad b_{5,r}=-\frac{1}{4}Pm\xi{f_r}'',\quad b_{6,r}=-\frac{1}{4}Pm\xi\frac{\partial\phi_r}{\partial\xi}-\frac{3}{4}Pm\phi_r,\quad b_{7,r}=-\frac{1}{4}Pm\xi\frac{\partial{\phi_r}'}{\partial\xi},$$

$$b_{8,r}=\frac{3}{4}Pm{\phi_r}'',\quad b_{9,r}=\frac{1}{4}Pm\xi{\phi_r}',\quad b_{10,r}=\frac{1}{4}\xi Pm{\phi_r}'',$$

$$c_{0,r}=1,\quad c_{1,r}=\frac{3}{4}Prf_r+\frac{1}{4}Pr\xi\frac{\partial f_r}{\partial\xi}+Pr\xi,\quad c_{2,r}=0,\quad c_{3,r}=-\frac{1}{4}Pr\xi{f_r}',\quad c_{4,r}=-\frac{1}{4}Pr\xi\frac{\partial\theta}{\partial\xi},$$

$$c_{5,r}=\frac{3}{4}Pr{\theta_r}',\quad c_{6,r}=\frac{1}{4}Pr\xi{\theta_r}',$$

$$R_{1,r}=\frac{3}{4}f_rf_r''-\frac{1}{2}({f_r}')^2-\frac{3}{4}S\phi_r\phi_r''+\frac{1}{2}S({\phi_r}')^2-\frac{1}{4}\xi{f_r}'\frac{\partial {f_r}'}{\partial\xi}+\frac{1}{4}\xi{f_r}''\frac{\partial f_r}{\partial\xi}+\frac{1}{4}\xi S{\phi_r}'\frac{\partial{\phi_r}'}{\partial\xi}-\frac{1}{4}\xi S{\phi_r}''\frac{\partial f_r}{\partial\xi}$$

$$R_{2,r}=\frac{3}{4}Pmf_r{\phi_r}''-\frac{3}{4}Pm{f_r}''\phi_r-\frac{1}{4}Pm\xi{f_r}'\frac{\partial{\phi_r}'}{\partial\xi}+\frac{1}{4}Pm\xi{\phi_r}'\frac{\partial{f_r}'}{\partial\xi}-\frac{1}{4}Pm\xi{f_r}''\frac{\partial\phi_r}{\partial\xi}+\frac{1}{4}Pm\xi{\phi_r}''\frac{\partial f_r}{\partial\xi}$$

$$R_{3,r}=\tfrac{3}{4}Prf_r{\theta_r}'-\tfrac{1}{4}Pr\xi{f_r}'\tfrac{\partial\theta_r}{\partial\xi}+\tfrac{1}{4}Pr\xi{\theta_r}'\tfrac{\partial f_r}{\partial\xi}. \quad (34)$$

To apply the multi-domain on ξ direction to the system of equations, we let $\xi\in\Omega$, where $\Omega\in[0,T]$ and the domain Ω is decomposed into p non-overlapping intervals as

$$\Omega_m=[\xi_{m-1},\xi_m],\xi_{m-1}<\xi_m,\xi_0=0,\xi_p=T,\quad m=1,2,\cdots,p. \quad (35)$$

The multi-domain approach is based on the assumption that the PDEs are solved independently at each of the p sub-interval using the initial condition for the solution in the first sub-interval. Once the solution at the first sub-interval has been computed, the new solutions at the subsequent $m-th$ interval is computed using the solution at the right hand boundary of the $m-1st$ interval as an initial solution. In the $m-th$ sub-interval, we solve

$$a_{0,r}^{(m)}{f'''}_{r+1}^{(m)} + a_{1,r}^{(m)}{f_{r+1}}''^{(m)} + a_{2,r}^{(m)}{f_{r+1}}'^{(m)} + a_{3,r}^{(m)}f_{r+1}^{(m)} + a_{4,r}^{(m)}\frac{\partial {f'}_{r+1}^{(m)}}{\partial\xi} + a_{5,r}^{(m)}\frac{\partial f_{r+1}^{(m)}}{\partial\xi} + a_{6,r}^{(m)}{\phi_{r+1}}''^{(m)} + a_{7,r}^{(m)}{\phi_{r+1}}'^{(m)} + a_{8,r}^{(m)}\phi_{r+1}^{(m)} + a_{9,r}^{(m)}\frac{\partial {\phi'}_{r+1}^{(m)}}{\partial\xi} + a_{10,r}^{(m)}\frac{\partial\phi_{r+1}^{(m)}}{\partial\xi} + a_{11,r}^{(m)}\theta_{r+1}^{(m)} = R_{1,r}^{(m)}, \quad (36)$$

$$b_{0,r}^{(m)}{\phi_{r+1}}'''^{(m)} + b_{1,r}^{(m)}{\phi_{r+1}}''^{(m)} + b_{2,r}^{(m)}{\phi_{r+1}}'^{(m)} + b_{3,r}^{(m)}\phi_{r+1}^{(m)} + b_{4,r}^{(m)}\frac{\partial {\phi'}_{r+1}^{(m)}}{\partial\xi} + b_{5,r}^{(m)}\frac{\partial\phi_{r+1}^{(m)}}{\partial\xi} + b_{6,r}^{(m)}{f_{r+1}}''^{(m)} + b_{7,r}^{(m)}{f_{r+1}}'^{(m)} + b_{8,r}^{(m)}f_{r+1}^{(m)} + b_{9,r}^{(m)}\frac{\partial {f'}_{r+1}^{(m)}}{\partial\xi} + b_{10,r}^{(m)}\frac{\partial f_{r+1}^{(m)}}{\partial\xi} = R_{2,r}^{(m)}, \quad (37)$$

$$c_{0,r}^{(m)}\theta_{r+1}{}''^{(m)} + c_{1,r}^{(m)}\theta_{r+1}{}'^{(m)} + c_{2,r}^{(m)}\theta_{r+1}^{(m)} + c_{3,r}^{(m)}\frac{\partial\theta_{r+1}^{(m)}}{\partial\xi} + c_{4,r}^{(m)}f_{r+1}{}'^{(m)} + c_{5,r}^{(m)}f_{r+1}^{(m)} + c_{6,r}^{(m)}\frac{\partial f_{r+1}^{(m)}}{\partial\xi} = R_{3,r}^{(m)}, \quad (38)$$

subject to the boundary conditions

$$f_{r+1}^{(m)}(0,\xi) = 0, f_{r+1}{}'^{(m)}(0,\xi) = 0, f_{r+1}{}'^{(m)}(\infty,\xi) = 0,$$
$$\phi_{r+1}^{(m)}(0,\xi) = 0, \phi_{r+1}{}'^{(m)}(0,\xi) = 1, \phi_{r+1}{}'^{(m)}(\infty,\xi) = 0,$$
$$\theta_{r+1}^{(m)}(0,\xi) = 1, \theta_{r+1}^{(m)}(\infty,\xi) = 0, \quad (39)$$

A suitable initial condition to start the multi-domain iteration scheme in the first sub-interval is on which satisfies the boundary conditions. Initial condition at the subsequent sub-intervals are given by the continuity conditions

$$f^{(m)}(\eta,\xi_{m-1}) = f^{(m-1)}(\eta,\xi_{m-1}),$$
$$\phi^{(m)}(\eta,\xi_{m-1}) = \phi^{(m-1)}(\eta,\xi_{m-1}),$$
$$\theta^{(m)}(\eta,\xi_{m-1}) = \theta^{(m-1)}(\eta,\xi_{m-1}). \quad (40)$$

Applying the spectral collocation method on above equations gives

$$\left[a_{0,r}^{(m)}D^3 + a_{1,r}^{(m)}D^2 + a_{2,r}^{(m)}D + a_{3,r}^{(m)}\right]F_{j,r+1}^{(m)} + a_{4,r}^{(m)}\sum_{q=0}^{N_t} d_{j,q}DF_{q,r+1}^{(m)} + a_{5,r}^{(m)}\sum_{q=0}^{N_t} d_{j,q}F_{q,r+1}^{(m)}$$
$$\left[a_{6,r}^{(m)}D^2 + a_{7,r}^{(m)}D + a_{8,r}^{(m)}\right]\boldsymbol{\Phi}_{j,r+1}^{(m)} + a_{9,r}^{(m)}\sum_{q=0}^{N_t} d_{j,q}D\boldsymbol{\Phi}_{q,r+1}^{(m)} + a_{10,r}^{(m)}\sum_{q=0}^{N_t} d_{j,q}\boldsymbol{\Phi}_{q,r+1}^{(m)}$$
$$+a_{11,r}^{(m)}\boldsymbol{\theta}_{j,r+1}^{(m)} = R_{1,j,r}^{(m)}, \quad (41)$$

$$\left[b_{0,r}^{(m)}D^3 + b_{1,r}^{(m)}D^2 + b_{2,r}^{(m)}D + b_{3,r}^{(m)}\right]\boldsymbol{\Phi}_{j,r+1}^{(m)} + b_{4,r}^{(m)}\sum_{q=0}^{N_t} d_{j,q}D\boldsymbol{\Phi}_{q,r+1}^{(m)} + b_{5,r}^{(m)}\sum_{q=0}^{N_t} d_{j,q}\boldsymbol{\Phi}_{q,r+1}^{(m)}$$
$$\left[b_{6,r}^{(m)}D^2 + b_{7,r}^{(m)}D + b_{8,r}^{(m)}\right]F_{j,r+1}^{(m)} + b_{9,r}^{(m)}\sum_{q=0}^{N_t} d_{j,q}DF_{q,r+1}^{(m)} + b_{10,r}^{(m)}\sum_{q=0}^{N_t} d_{j,q}F_{q,r+1}^{(m)} = R_{2,j,r}^{(m)}, \quad (42)$$

$$\left[c_{0,r}^{(m)}D^2 + c_{1,r}^{(m)}D + c_{2,r}^{(m)}\right]\boldsymbol{\Theta}_{j,r+1}^{(m)} + c_{3,r}^{(m)}\sum_{q=0}^{N_t} d_{j,q}\boldsymbol{\Theta}_{q,r+1}^{(m)} + \left[c_{4,r}^{(m)}D + c_{5,r}^{(m)}\right]F_{j,r+1}^{(m)}$$
$$+c_{6,r}^{(m)}\sum_{q=0}^{N_t} d_{j,q}F_{q,r+1}^{(m)} = R_{3,j,r}^{(m)}. \quad (43)$$

Noting that the solution at the last time level $j = N_t$ of each sub-interval is given by the initial condition and taking i and j now as dummy indices, it can be written as

$$\left[a_{0,r}^{(m)}D^3 + a_{1,r}^{(m)}D^2 + a_{2,r}^{(m)}D + a_{3,r}^{(m)}\right]F_{i,r+1}^{(m)} + a_{4,r}^{(m)}\sum_{j=0}^{N_t-1} d_{i,j}DF_{j,r+1}^{(m)} + a_{5,r}^{(m)}\sum_{j=0}^{N_t-1} d_{i,j}F_{j,r+1}^{(m)}$$
$$+\left[a_{6,r}^{(m)}D^2 + a_{7,r}^{(m)}D + a_{8,r}^{(m)}\right]\boldsymbol{\Phi}_{i,r+1}^{(m)} + a_{9,r}^{(m)}\sum_{j=0}^{N_t-1} d_{i,j}D\boldsymbol{\Phi}_{j,r+1}^{(m)} + a_{10,r}^{(m)}\sum_{j=0}^{N_t-1} d_{i,j}\boldsymbol{\Phi}_{j,r+1}^{(m)} + a_{11,r}^{(m)}\boldsymbol{\theta}_{j,r+1}^{(m)}$$
$$= R_{1,i,r}^{(m)} - a_{4,r}^{(m)}d_{i,N_t}DF_{N_t,r+1}^{(m)} + a_{5,r}^{(m)}d_{i,N_t}F_{N_t,r+1}^{(m)} - a_{9,r}^{(m)}d_{i,N_t}D\boldsymbol{\Phi}_{N_t,r+1}^{(m)} - a_{10,r}^{(m)}d_{i,N_t}\boldsymbol{\Phi}_{N_t,r+1}^{(m)}, \quad (44)$$

$$\left[b_{0,r}^{(m)}D^3 + b_{1,r}^{(m)}D^2 + b_{2,r}^{(m)}D + b_{3,r}^{(m)}\right]\boldsymbol{\Phi}_{i,r+1}^{(m)} + b_{4,r}^{(m)}\sum_{j=0}^{N_t-1} d_{i,j}D\boldsymbol{\Phi}_{j,r+1}^{(m)} + b_{5,r}^{(m)}\sum_{j=0}^{N_t-1} d_{i,j}\boldsymbol{\Phi}_{j,r+1}^{(m)}$$
$$+\left[b_{6,r}^{(m)}D^2 + b_{7,r}^{(m)}D + b_{8,r}^{(m)}\right]F_{i,r+1}^{(m)} + b_{9,r}^{(m)}\sum_{j=0}^{N_t-1} d_{i,j}DF_{j,r+1}^{(m)} + b_{10,r}^{(m)}\sum_{j=0}^{N_t-1} d_{i,j}F_{j,r+1}^{(m)}$$
$$= R_{2,i,r}^{(m)} - b_{4,r}^{(m)}d_{i,N_t}D\boldsymbol{\Phi}_{N_t,r+1}^{(m)} - b_{5,r}^{(m)}d_{i,N_t}\boldsymbol{\Phi}_{N_t,r+1}^{(m)} - b_{9,r}^{(m)}d_{i,N_t}DF_{N_t,r+1}^{(m)} - b_{10,r}^{(m)}d_{i,N_t}F_{N_t,r+1}^{(m)}, \quad (45)$$

$$\left[c_{0,r}^{(m)}D^2 + c_{1,r}^{(m)}D + c_{2,r}^{(m)}\right]\boldsymbol{\Theta}_{i,r+1}^{(m)} + c_{3,r}^{(m)}\sum_{j=0}^{N_t-1} d_{i,j}\boldsymbol{\Theta}_{j,r+1}^{(m)} + \left[c_{4,r}^{(m)}D + c_{5,r}^{(m)}\right]F_{i,r+1}^{(m)} + c_{6,r}^{(m)}\sum_{j=0}^{N_t-1} d_{i,j}F_{q,r+1}^{(m)}$$
$$= R_{3,i,r}^{(m)} - c_{3,r}^{(m)}d_{i,N_t}\boldsymbol{\Theta}_{N_t,r+1}^{(m)} - c_{6,r}^{(m)}d_{i,N_t}F_{N_t,r+1}^{(m)}. \quad (46)$$

In a more compact form, thse equations can be written as

$$A_{1,1}^{(i)}F_{i,r+1}^{(m)} + a_{4,r}^{(m)}\sum_{j=0}^{N_t-1} d_{i,j}DF_{j,r+1}^{(m)} + a_{5,r}^{(m)}\sum_{j=0}^{N_t-1} d_{i,j}F_{j,r+1}^{(m)} + A_{1,2}^{(i)}\boldsymbol{\Phi}_{i,r+1}^{(m)} + a_{9,r}^{(m)}\sum_{j=0}^{N_t-1} d_{i,j}D\boldsymbol{\Phi}_{j,r+1}^{(m)} + a_{10,r}^{(m)}\sum_{j=0}^{N_t-1} d_{i,j}\boldsymbol{\Phi}_{j,r+1}^{(m)} + A_{1,3}^{(i)}\boldsymbol{\Theta}_{i,r+1}^{(m)} = \boldsymbol{\beta}_{1,i,r}^{(m)}, \quad (47)$$

$$A_{2,1}^{(i)}F_{i,r+1}^{(m)} + b_{9,r}^{(m)}\sum_{j=0}^{N_t-1} d_{i,j}DF_{j,r+1}^{(m)} + b_{10,r}^{(m)}\sum_{j=0}^{N_t-1} d_{i,j}F_{j,r+1}^{(m)} + A_{2,2}^{(i)}\boldsymbol{\Phi}_{i,r+1}^{(m)} + b_{4,r}^{(m)}\sum_{j=0}^{N_t-1} d_{i,j}D\boldsymbol{\Phi}_{j,r+1}^{(m)} + b_{5,r}^{(m)}\sum_{j=0}^{N_t-1} d_{i,j}\boldsymbol{\Phi}_{j,r+1}^{(m)} + A_{2,3}^{(i)}\boldsymbol{\Theta}_{i,r+1}^{(m)} = \boldsymbol{\beta}_{2,i,r}^{(m)}, \quad (48)$$

$$A_{3,1}^{(i)}F_{i,r+1}^{(m)} + c_{6,r}^{(m)}\sum_{j=0}^{N_t-1} d_{i,j}F_{j,r+1}^{(m)} + A_{3,2}^{(i)}\boldsymbol{\Phi}_{i,r+1}^{(m)} + A_{3,3}^{(i)}\boldsymbol{\Theta}_{i,r+1}^{(m)} + c_{3,r}^{(m)}\sum_{j=0}^{N_t-1} d_{i,j}\boldsymbol{\Theta}_{j,r+1}^{(m)} = \boldsymbol{\beta}_{3,i,r}^{(m)}, \quad (49)$$

where

$$A_{1,1}^{(i)} = a_{0,r}^{(m)}D^3 + a_{1,r}^{(m)}D^2 + a_{2,r}^{(m)}D + a_{3,r}^{(m)}, A_{1,2}^{(i)} = a_{6,r}^{(m)}D^2 + a_{7,r}^{(m)}D + a_{8,r}^{(m)}, A_{1,3}^{(i)} = a_{11,r}^{(m)}$$

$$A_{2,1}^{(i)} = b_{6,r}^{(m)}D^2 + b_{7,r}^{(m)}D + b_{8,r}^{(m)}, A_{2,2}^{(i)} = b_{0,r}^{(m)}D^3 + b_{1,r}^{(m)}D^2 + b_{2,r}^{(m)}D, +b_{3,r}^{(m)}A_{2,3}^{(i)} = \mathbf{0}$$

$$A_{3,1}^{(i)} = c_{4,r}^{(m)}D + c_{5,r}^{(m)}, A_{3,2}^{(i)} = \mathbf{0}, A_{3,3}^{(i)} = c_{0,r}^{(m)}D^2 + c_{1,r}^{(m)}D, +c_{2,r}^{(m)}$$

$$\boldsymbol{\beta}_{1,i,r}^{(m)} = R_{1,i,r}^{(m)} - a_{4,r}^{(m)}d_{i,N_t}DF_{N_t,r+1}^{(m)} - a_{5,r}^{(m)}d_{i,N_t}F_{N_t,r+1}^{(m)} - a_{9,r}^{(m)}d_{i,N_t}D\boldsymbol{\Phi}_{N_t,r+1}^{(m)} - a_{10,r}^{(m)}d_{i,N_t}\boldsymbol{\Phi}_{N_t,r+1}^{(m)},$$

$$\boldsymbol{\beta}_{2,i,r}^{(m)} = R_{2,i,r}^{(m)} - b_{4,r}^{(m)}d_{i,N_t}D\boldsymbol{\Phi}_{N_t,r+1}^{(m)} - b_{5,r}^{(m)}d_{i,N_t}\boldsymbol{\Phi}_{N_t,r+1}^{(m)} - b_{9,r}^{(m)}d_{i,N_t}DF_{N_t,r+1}^{(m)} - b_{10,r}^{(m)}d_{i,N_t}F_{N_t,r+1}^{(m)},$$

$$\boldsymbol{\beta}_{3,i,r}^{(m)} = R_{3,i,r}^{(m)} - c_{3,r}^{(m)}d_{i,N_t}\boldsymbol{\Theta}_{N_t,r+1}^{(m)} - c_{6,r}^{(m)}d_{i,N_t}F_{N_t,r+1}^{(m)}.$$

The boundary conditions when evaluated at the Chebyshev-Gauss-Lobatto collocation points gives:

$$f_{r+1}^{(m)}(\eta_{N_x},\xi_i) = 0, \sum_{p=0}^{N_x} D_{N_x,p}f_{r+1}^{(m)}(N_x,\xi_i) = 0, \sum_{p=0}^{N_x} D_{0,p}f_{r+1}^{(m)}(\eta_p,\xi_i) = 0,$$

$$\phi_{r+1}^{(m)}(\eta_{N_x},\xi_i) = 0, \sum_{p=0}^{N_x} D_{N_x,p}\phi_{r+1}^{(m)}(N_x,\xi_i) = 1, \sum_{p=0}^{N_x} D_{0,p}\phi_{r+1}^{(m)}(\eta_p,\xi_i) = 0,$$

$$\theta_{r+1}^{(m)}(\eta_{N_x},\xi_i) = 1, \theta_{r+1}^{(m)}(\eta_0,\xi_i) = 0. \quad (50)$$

Solving these equations gives $f(x_p,t_q)$, $\phi(x_p,t_q)$ and $\theta(x_p,t_q)$ which is subsequently used to approximate $f^m(x,t)$, $\phi^m(x,t)$, and $\theta^m(x,t)$.

5. RESULTS AND DISCUSSIONS

In this section, we present the numerical approximate solutions for equations (1 - 3), subject to the boundary conditions (4) obtained using the large parameter spectral perturbation method (LSPM). Results were presented for the skin friction coefficient $(f''(0,\xi))$, rate of heat transfer $(-\theta'(0,\xi))$ and the current density $(-\phi''(0,\xi))$ for different physical parameters that are of interest to the flow model. To ascertain the accuracy of the computed (LSPM) approximate numerical results comparison was done against numerical approximate results obtained using the multi-domain bivariate spectral quasilinearisation method (MD-BSQLM) and the results were seen to be in a very good agreement. For the LSPM, the number of collocation points used in the space (η) direction is $N_x = 100$ in all cases. Similarly, for the MD-BSQLM, the number of collocation points used in the space (η) direction to generate the numerical results is $N_x = 100$ and in the (ξ) direction is $N_t = 5$ in all cases. The choice of these collocation points gave the sufficient accuracy required in all the numerical simulations conducted.

Table-1, illustrates a comparison of the approximate numerical results of equations (1 - 3) computed by the (LSPM) and the (MD-BSQLM) for the skin friction $f''(0,\xi)$, current density $-\phi''(0,\xi)$ and rate of heat transfer $-\theta'(0,\xi)$, respectively, for different values of the transpiration parameter (ξ) when the magnetic Prandtl number $Pm = 0.7$, magnetic field parameter $S = 0.2$, and Prandtl number $Pr = 0.7$. The table also gives the order (K) of LSPM approximation and the (LSPM) and the (MD-BSQLM) computational time required to obtain numerical results that are accurate to seven decimal places. It can be seen from the table that the (LSPM) results are found to be in excellent agreement with the result of the (MD-BSQLM). It is worth mentioning here that the asymptotic series solution of equations (1 - 3) are presented by Ashraf *et al.* [1], where tabulated results for $F''(0)$, $\Phi''(0)$ and $\Theta(0)$ when $Pm = 0.01,0.05,0.1$, $S = 0.2$, and $Pr = 0.1$ for different values of ξ. We have decided not to compare our present results with the reported results of Ashraf *et al.* [1] because an incorrect transformation for equation (2) was used in their study. Here, we have reported the correct transformation and equations. It can further be observed from the table that converged solutions are reached at very low LSPM order when ξ is very large. More terms of the series are required to give converged results when ξ is small. The comparison between the computational times shows that the (LSPM) is more efficient in terms of computation speed than the (MD-BSQLM). It is worth mentioning that the apparent computational speed of the LSPM can be explained by the fact that, unlike the MD-BSQLM, discretization is done only in the space (η) direction in the LSPM. From this Table, it is also observed

that an increase in the values of transpiration parameter ξ, decreases the skin friction but increases the current density and rate of heat transfer.

Figures 1, 2 and 3 show the effects of the transpiration parameter ξ on the velocity profile $f'(\eta,\xi)$, the transverse component of magnetic field $\phi(\eta,\xi)$ and the temperature profile $\theta(\eta,\xi)$, respectively. From the graphs, it can be seen that the velocity profile, the transverse component of the magnetic field and the temperature profile decreases as the transpiration parameter ξ increases. It can be further noticed that the momentum, magnetic and thermal boundary layer thickness decreases with increasing values of ξ. This phenomenon occurs because suction slows down the motion of the fluid in the downstream region. Similar observations were made in a parallel study by [1] and [15]. Figures 4 and 5, presents the effect of the magnetic on the velocity profile and transverse component of magnetic field. We observe from the graphs that an increase in the values of the magnetic field parameter leads to an increase in the velocity profile, and in the transverse component of magnetic field. This is because the direction of the magnetic field is in favour of the temperature profile. Similar results have been reported in a parallel study carried out by [15].

Figures 6 and 7 illustrates the effect of magnetic Prandtl number Pm on the velocity profile and transverse component of magnetic field, and temperature profile respectively. From these Figures, it can be seen that both velocity profile and transverse component of magnetic field decreases while there is no change noticed on the temperature profile. Similar observations on transverse component of magnetic field and temperature profile were made in a parallel study by [15].

The velocity and temperature profiles for various values of the Prandtl number Pr are displayed in Figures 8 and 9. It is noted that both the velocity and temperature decreases. We further observe that the momentum and thermal boundary layer thickness decreases with the increase in the values of Pr. This happens because an increase in the Prandtl number implies an increase in the fluid viscosity, which in turn, causes a reduction in the velocity and temperature profiles. These results agree with those of a parallel study carried out by [15].

In order to further access the accuracy of the LSPM numerical method, we have considered the residual error which is a representation of the extent at which the solution of the governing partial differential equations (7 - 9) is approximated by the numerical solution. Accordingly, we define the residual error as we define the maximum error of the residual as

$$Res(F) = \max_{0\le j\le N_x} |\bar{N}_F[F_k(\xi,\eta),\boldsymbol{\Phi}_k(\xi,\eta),\boldsymbol{\Theta}_k(\xi,\eta)]|,$$
$$Res(\Phi) = \max_{0\le j\le N_x} |\bar{N}_\Phi[F_k(\xi,\eta),\boldsymbol{\Phi}_k(\xi,\eta),\boldsymbol{\Theta}_k(\xi,\eta)]|,$$
$$Res(\Theta) = \max_{0\le j\le N_x} |\bar{N}_\Theta[F_k(\xi,\eta),\boldsymbol{\Phi}_k(\xi,\eta),\boldsymbol{\Theta}_k(\xi,\eta)]|, \quad (51)$$

where $\bar{N}_F, \bar{N}_\Phi$ and $\bar{N}_\Theta$ are the governing nonlinear PDEs defined as

$$\bar{N}_F = F''' + F'' + \Theta - \frac{1}{2}S\Phi\Phi'' + \frac{1}{2}S\Phi'^2 - \frac{1}{4}\xi^{-3}\left[F'^{\frac{\partial F'}{\partial\xi}} - F''^{\frac{\partial F}{\partial\xi}}\right] + \frac{1}{4}\xi S\left[\Phi'\frac{\partial\Phi'}{\partial\xi} - \Phi''\frac{\partial\Phi}{\partial\xi}\right],$$

$$\bar{N}_\Phi = \Phi''' + Pm\Phi'' - \frac{1}{2}Pm\xi^{-4}F''\Phi - \frac{1}{2}Pm\xi^{-4}F'\Phi' - \frac{1}{4}Pm\xi^{-3}\left[F'\frac{\partial\Phi'}{\partial\xi} - \Phi'\frac{\partial F'}{\partial\xi} + F''\frac{\partial\Phi}{\partial\xi} - \Phi''\frac{\partial F}{\partial\xi}\right],$$

$$\bar{N}_\Theta = \Theta'' + Pr\Theta' - \frac{1}{4}Pr\xi^{-3}\left[F'\frac{\partial\Theta}{\partial\xi} - \Theta'\frac{\partial F}{\partial\xi}\right].$$

and $F_k(\xi,\eta), \boldsymbol{\Phi}_k(\xi,\eta), \text{and}\boldsymbol{\Theta}_k(\xi,\eta)$ are the LSPM approximate solutions.

Figures 10, 11 and 12 depict the variation of the LSPM residual error for F, Φ and Θ against increasing order of the LSPM series term. From the graph, it can be observed that the residual error reduces with an increase in the order of LSPM series approximation for different values of ξ considered. The decrease in the residual error slope with an incraese in the order of series approximation is an indication that the method converges and the convergence is observed to be linear. We also note that for very large values of ξ, convergence improves, and convergence is attained with just a few terms of the LSPM approximation. This is because the series expansion is inversely proportional to ξ, therefore, it is expected that the accuracy of the method will improve as ξ becomes large. The saturation level is at least 10^{-9} for $F(\eta,\xi)$ equation, and about 10^{-11} in the equations for $\Phi(\eta,\xi)$ and $\Theta(\eta,\xi)$.

6. CONCLUSIONS

This paper has considered the application of the large parameter spectral perturbation method (LSPM) in the solution of nonlinear boundary layer partial differential equations. The (LSPM) algorithm was developed by coupling the analytical idea with numerical analysis and solving the resulting system of equations generated by the series approximation using the Chebyshev spectral collocation method. The proposed (LSPM) was used to solve a system of three previously reported nonlinear partial differential equations that model boundary layer flow problems. The accuracy and validity of the LSPM were tested against multi-domain bivariate interpolated spectral quasilinearisation method (MD-BSQLM) which is a numerical method that blends the Newton-Raphson based quasilinearisation idea of linearising systems of equations and Chebyshev spectral collocation with bivariate Lagrange interpolation to solve the resulting linearised system of equations on a sequence of multiple intervals. Graphical results were presented showing the

effects of different flow parameters on the velocity profile, the transverse component of magnetic field and the temperature profile. The observations made were found to be in good agreement with other results in similar studies reported in the literature. Numerical simulations were conducted in order to further access the accuracy, computational efficiency, and effectiveness of the method in solving nonlinear partial differential equations. It is obvious from the study that the (LSPM) gives approximate numerical solutions that are accurate and valid in large parameter domain in a computationally efficient manner. Further observation from this study is that the (LSPM) is significantly more computationally faster than the (MD-BSQLM). The numerical result presented in this study clearly demonstrate that the (LSPM) can be used as a numerical tool for numerical solutions of the boundary layer flows equations similar to the model equations investigated in this study. The study adds to the growing body of literature on numerical methods for solving coupled nonlinear partial differential equations arising in fluid mechanics that are defined over large domains.

ACKNOWLEDGMENT

This work is supported by the National Research Foundation of South Africa (Grant Number 116661) and the Durban University of Technology, South Africa.

REFERENCES

[1] M. Ashraf, S. Asghar, Z. Syed and M.A. Hossain. 2013. Natural Convection Heat Transfer Flow Past a Magnetized Vertical Permeable Plate for Liquid Metals, Middle-East J. of Scientific Research. 13: 983-992.

[2] M.M. Abd-Elaziz and S. E. Sameh. 2008. Group Solution for Unsteady Boundary Layer Flow of a Micropolar Fluid near the Rear Stagnation Point of a Plane Surface in a Porous Medium, Latin American Applied Research. 38: 161-168.

[3] S. Liao. 2006. Series Solutions of Unsteady Boundary-Layer Flows Over a Stretching Flat Plate, Studies in Applied Math.117: 239-263.

[4] M. Kumari and G. Nath. 1996. Boundary Layer Development on a Continuous Moving Surface with a Parallel Free Stream due to Impulsive Motion, Heat and Mass Transf.31: 283-289.

[5] S.S. Motsa, Z.G. Makukula and S. Shateyi. 2015. Numerical Investigation of the Effect of Unsteadiness on Three-Dimensional Flow of an Oldroyb-B Fluid, PloS one. Vol. 10, e0133507.

[6] S.S. Motsa and M.S. Ansari. 2015. Unsteady Boundary Layer Flow and Heat Transfer of Oldroyd-B Nanofluid towards a Stretching Sheet with Variable Thermal Conductivity, Thermal Sci. 19(suppl. 1): 239–248.

[7] S.S. Motsa and I.L. Animasaun. 2015. A New Numerical Investigation of some Thermo-physical Properties on Unsteady MHD Non-Darcian Flow Past an Impulsively Started Vertical Surface, Thermal Sci. 19(suppl. 1): 249-258.

[8] S.S. Motsa. 2014. On the Bivariate Spectral Homotopy Analysis Method Approach for Solving Nonlinear Evolution Partial Differential Equations, Abstract and Applied Analysis, vol. 2014, Article ID 350529, 8 pages, doi:10.1155/2014/350529.

[9] M.A. Hossain, M.S. Munir, M.Z. Hafiz and H.S. Takhar. 2000. Flow of a Viscous Incompressible Fluid of Temperature Dependent Viscosity Past a Permeable Wedge with Uniform Surface Heat Flux, Heat and Mass Transf. 36: 333-341.

[10] T.M. Agbaje and S.S. Motsa. 2015. Comparison between Spectral Perturbation and Spectral Relaxation Approach for Unsteady Heat and Mass Transfer by MHD Mixed Convection Flow Over an Impulsively Stretched Vertical Surface with Chemical Reaction Effect, J. of Interpolation and Approximation in Scientific Computing. 2015: 48-83.

[11] R.E. Bellman and R.E. Kalaba. 1965. Quasilinearization and Nonlinear Boundary-Value Problems, Elsevier Publishing Company, New York.

[12] H.S. Nik, and P. Rebelo. 2014. Multistage Spectral Relaxation Method for Solving the Hyperchaotic Complex Systems, The Scientific World J. 2014(Article ID 943293): 10, doi:10.1155/2014/943293, 2014.

[13] S. Effati, H.S. Nik and M. Shirazian. 2013. An Improvement to the Homotopy Perturbation Method for Solving the Hamilton–Jacobi–Bellman Equation, IMA J. of Mathematical Control and Info. 30: 487-506.

[14] S.M. Goh, M.S.M. Noorani and H. Ishak. 2010. On Solving the Chaotic Chen System: A New Time Marching Design for the Variational Iteration Method using Adomian's Polynomial, Numerical Algo. 54: 245-260.

[15] M. Ashraf, S. Asghar and M.A. Hossain. 2012. Computational Study of Combined Effects of

Conduction-radiation and Hydromagnetics on Natural Convection Flow past Magnetized Permeable Plate, Applied Math. Mech.33: 731-748.

Table-1. Comparison of the MD-BQLM and LSPM approximate numerical solutions of $f''(0,\xi)$, $-\phi''(0,\xi)$ and $-\theta'(0,\xi)$, for different values of ξ when $Pr = 0.7$, $Pm = 0.7$ and $S = 0.2$.

ξ	$f''(0,\xi)$			$-\phi''(0,\xi)$			$-\theta'(0,\xi)$		
	K	**LSPM**	**MD-BSQLM**	**K**	**LSPM**	**MD-BSQLM**	**K**	**LSPM**	**MD-BSQLM**
3	5	0.5238083	0.5237830	5	2.1000000	2.1000099	6	2.1000002	2.1000109
4	4	0.3928570	0.3928570	4	2.8000000	2.8000002	5	2.8000000	2.8000000
5	2	0.3142858	0.3142858	2	3.5000000	3.5000000	2	3.5000000	3.5000000
10	1	0.1571429	0.1571429	1	7.0000000	7.0000000	1	7.0000000	7.0000000
15	1	0.1047619	0.1047619	1	10.5000000	10.5000000	1	10.5000000	10.5000000
20	1	0.0785714	0.0785714	1	14.0000000	14.0000000	1	14.0000000	14.0000000
25	1	0.0628571	0.0628571	1	17.5000000	17.5000000	1	17.5000000	17.5000000
30	1	0.0523810	0.0523810	1	21.0000000	21.0000000	1	21.0000000	21.0000000
CPU Time		0.024995	9.771254		0.024995	9.771254		0.024995	9.771254

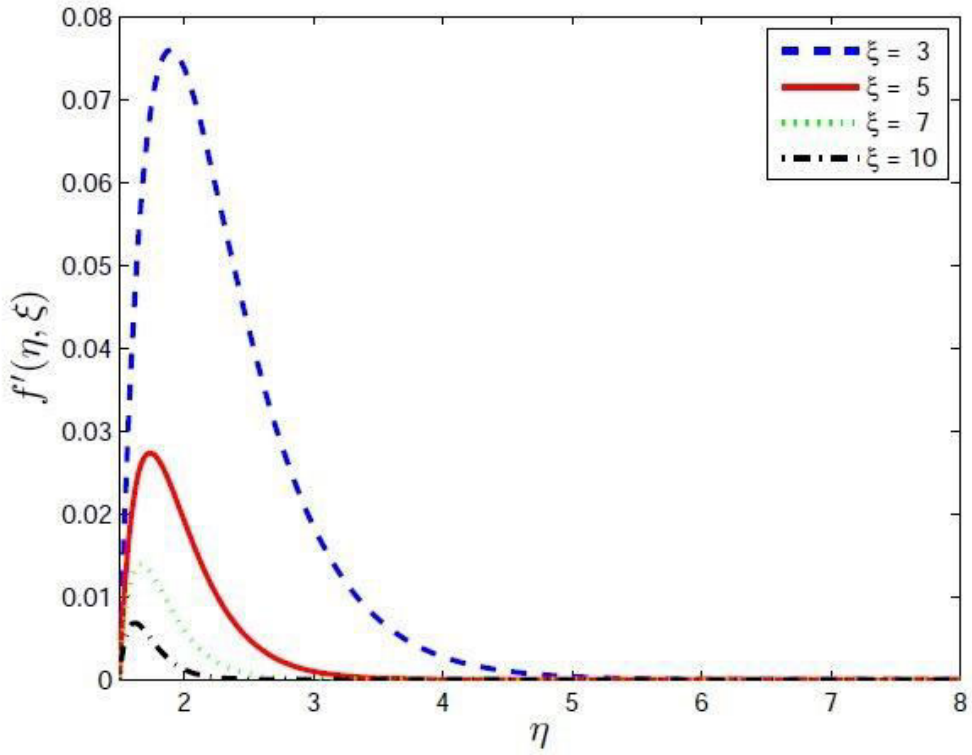

Figure-1. Velocity profile $f'(\eta,\xi)$ for different values of transpiration parameter ξ when $Pr = 0.7, S = 0.2, Pm = 0.7, N_x = 150,$ and$N_x = 60$.

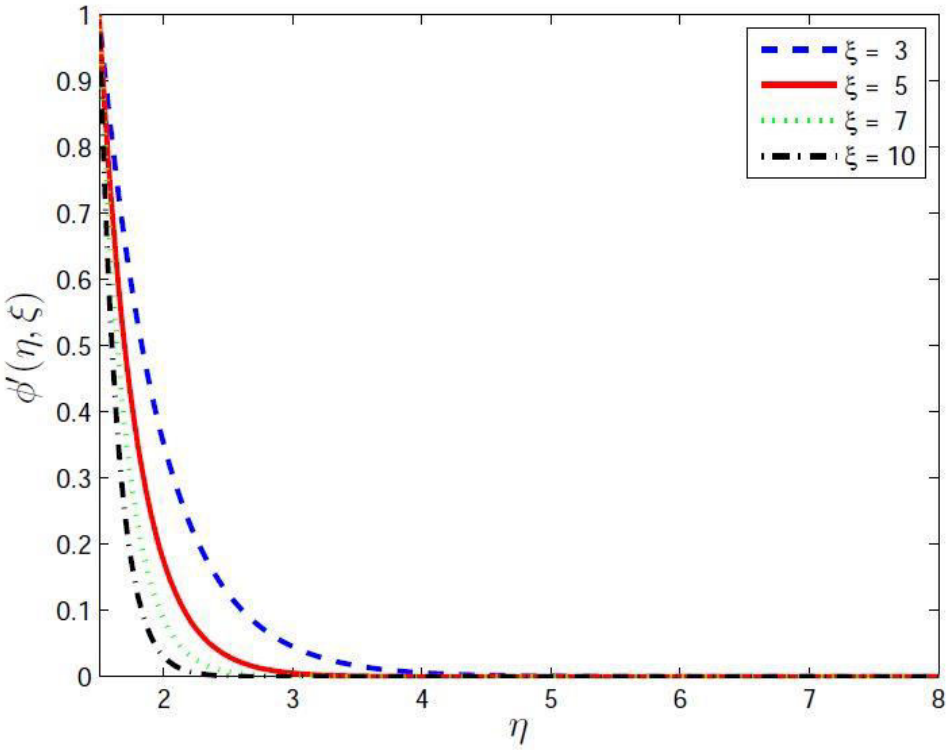

Figure-2. Transverse component of magnetic field $\phi'(\eta,\xi)$ for different transpiration parameter ξ when $Pr = 0.7, S = 0.2,$ and $Pm = 0.7$.

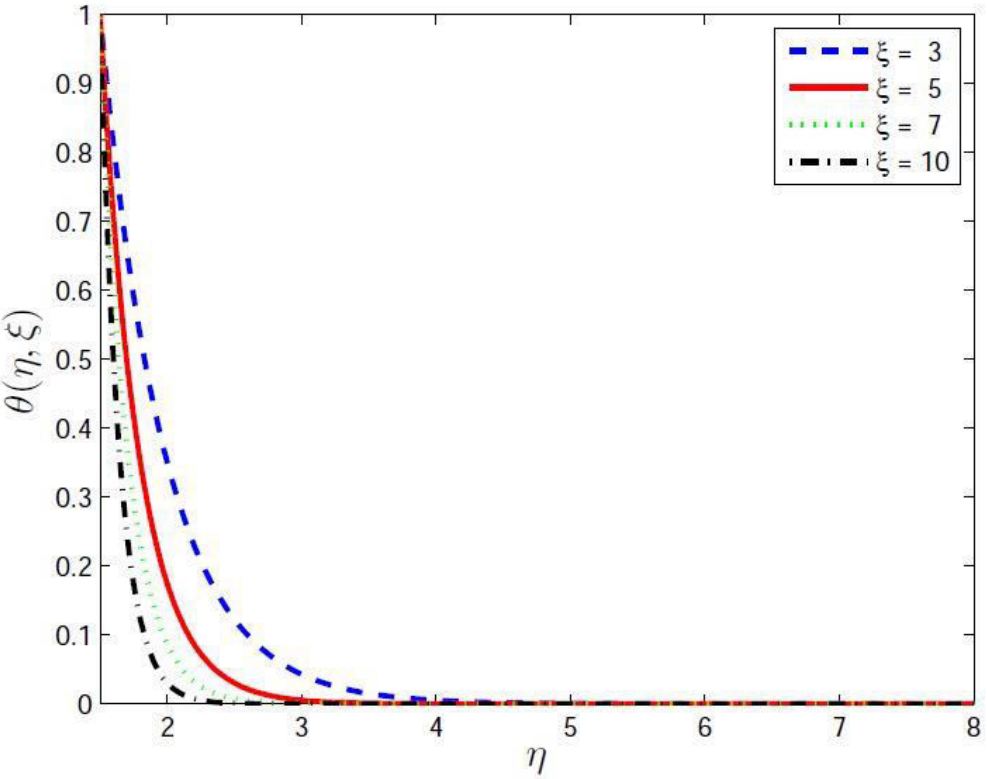

Figure-3. Temperature profile $\theta(\eta,\xi)$ for different values of transpiration parameter ξ when $Pr = 0.7, S = 0.2,$ and $Pm = 0.7$.

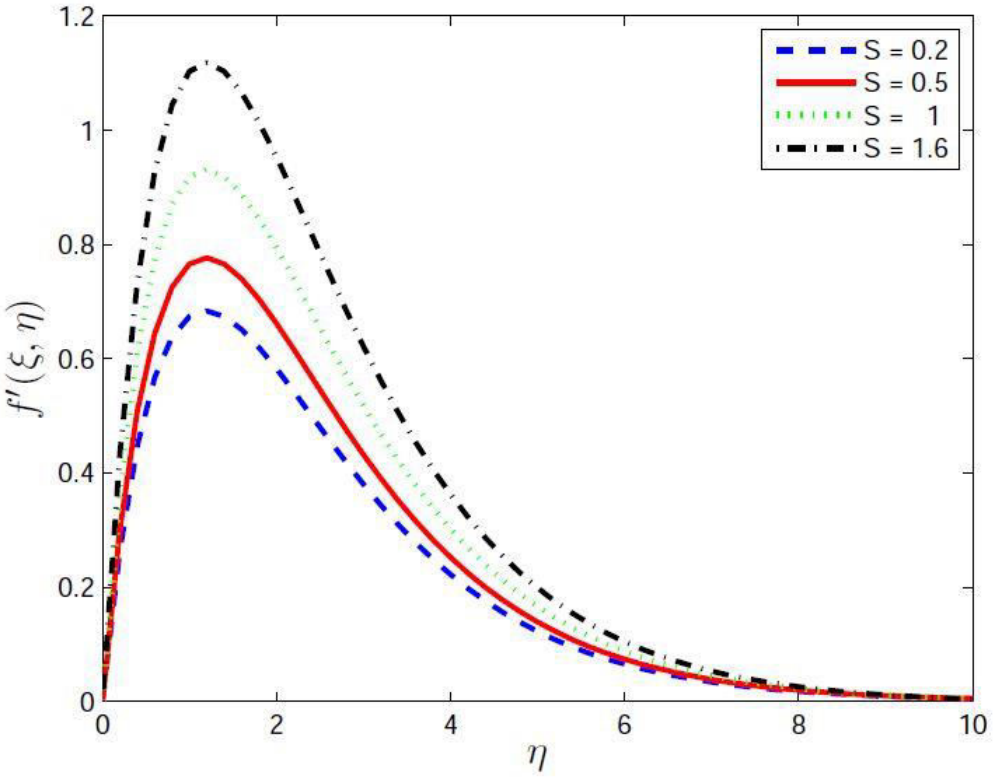

Figure-4. Velocity profile $f'(\eta,\xi)$ for different values of magnetic field parameter S when $Pr = 0.7, \xi = 2,$ and $Pm = 0.7$.

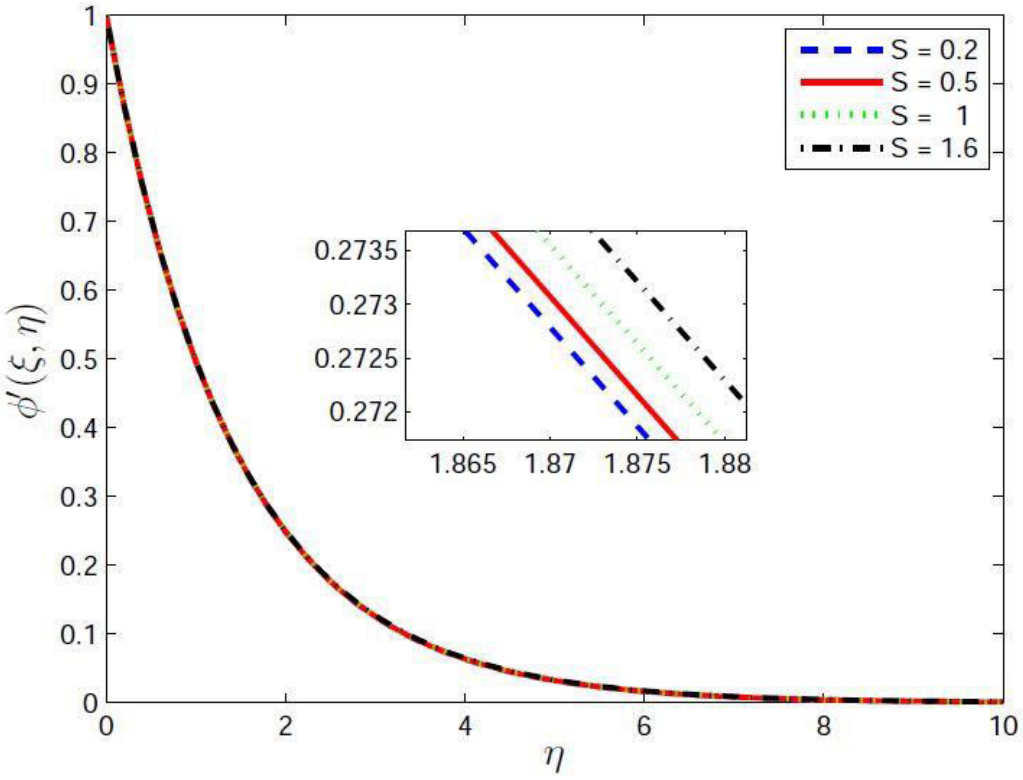

Figure-5. Transverse component of magnetic field $\phi'(\eta,\xi)$ for different values of magnetic field parameter S when $Pr = 0.7, \xi = 2,$ and $Pm = 0.7$.

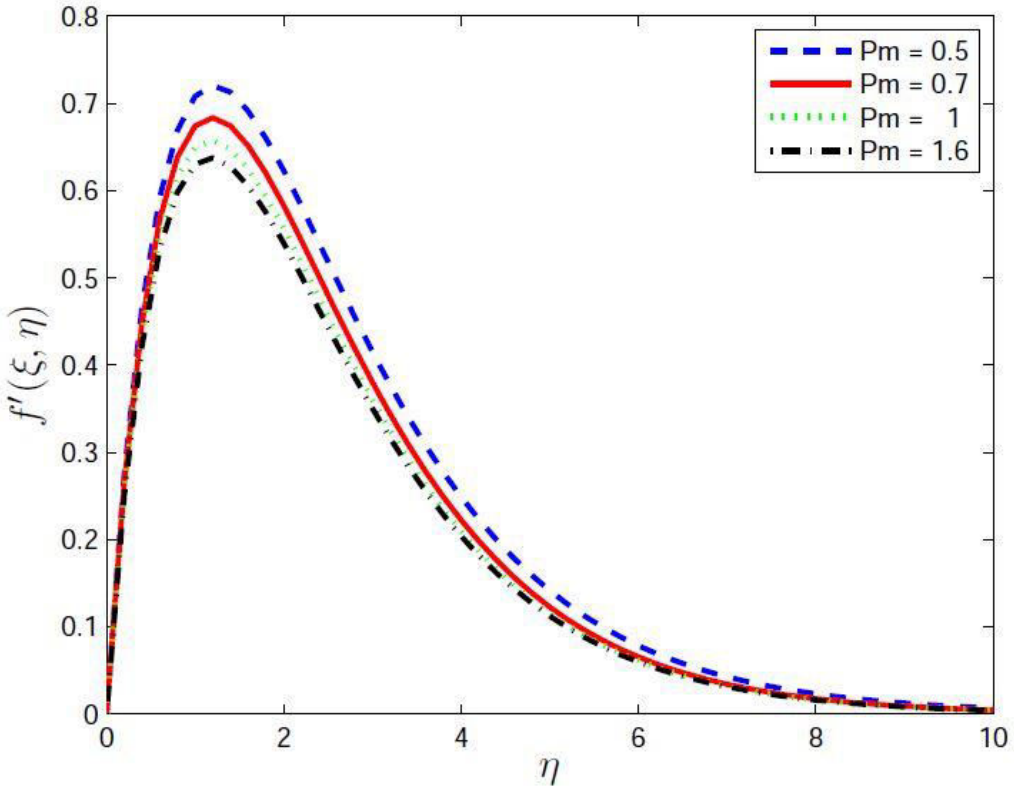

Figure-6. Velocity profile $f'(\eta,\xi)$ for different values of magnetic Prandtl number Pm when $Pr = 0.7, \xi = 2,$ and $S = 0.2$.

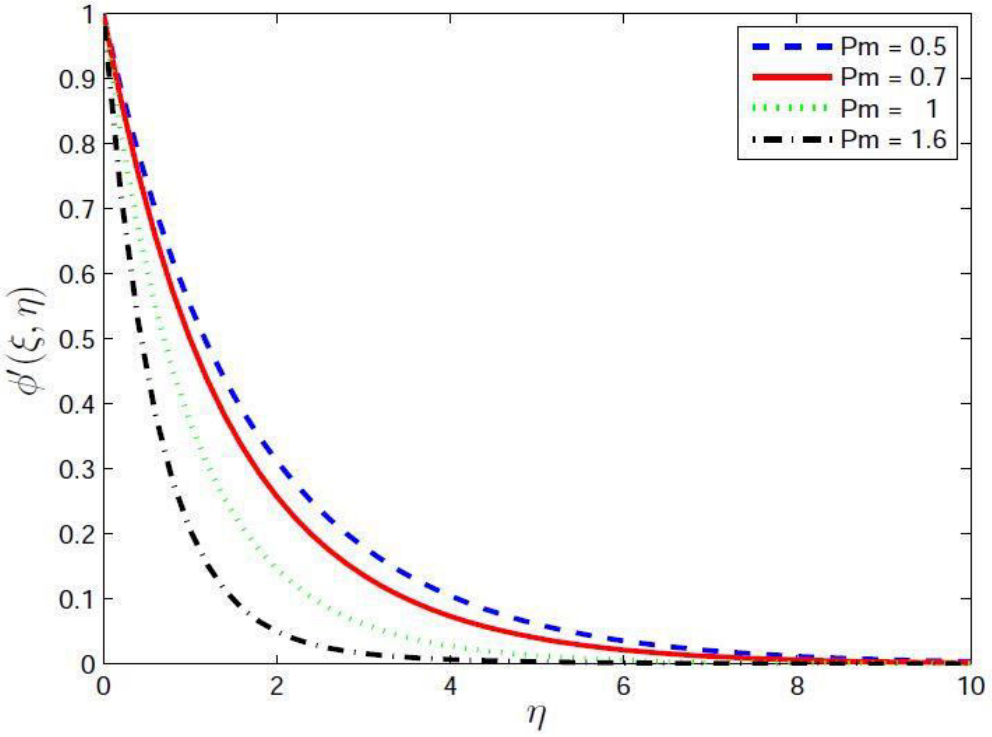

Figure-7. Transverse component of magnetic field $\phi'(\eta,\xi)$ for different values of magnetic Prandtl number Pm when $Pr = 0.7, \xi = 2,$ and $S = 0.2$.

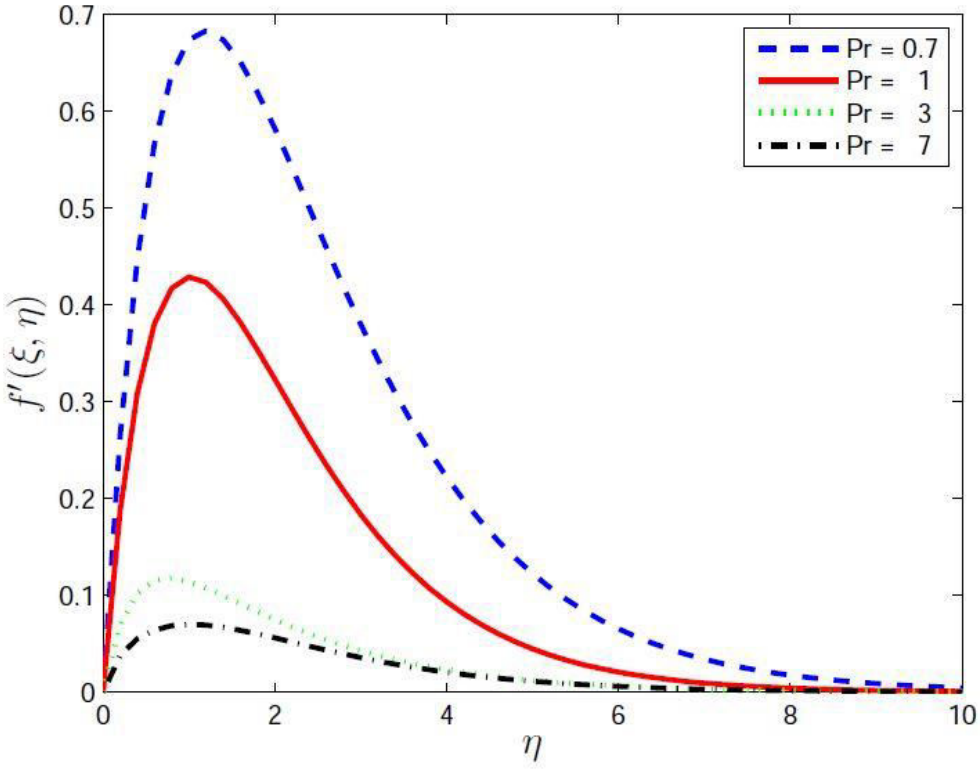

Figure-8. Velocity profile $f'(\eta,\xi)$ for different values of Prandtl number Pr when $Pm = 0.7,\quad \xi = 2,$ and $S = 0.2$.

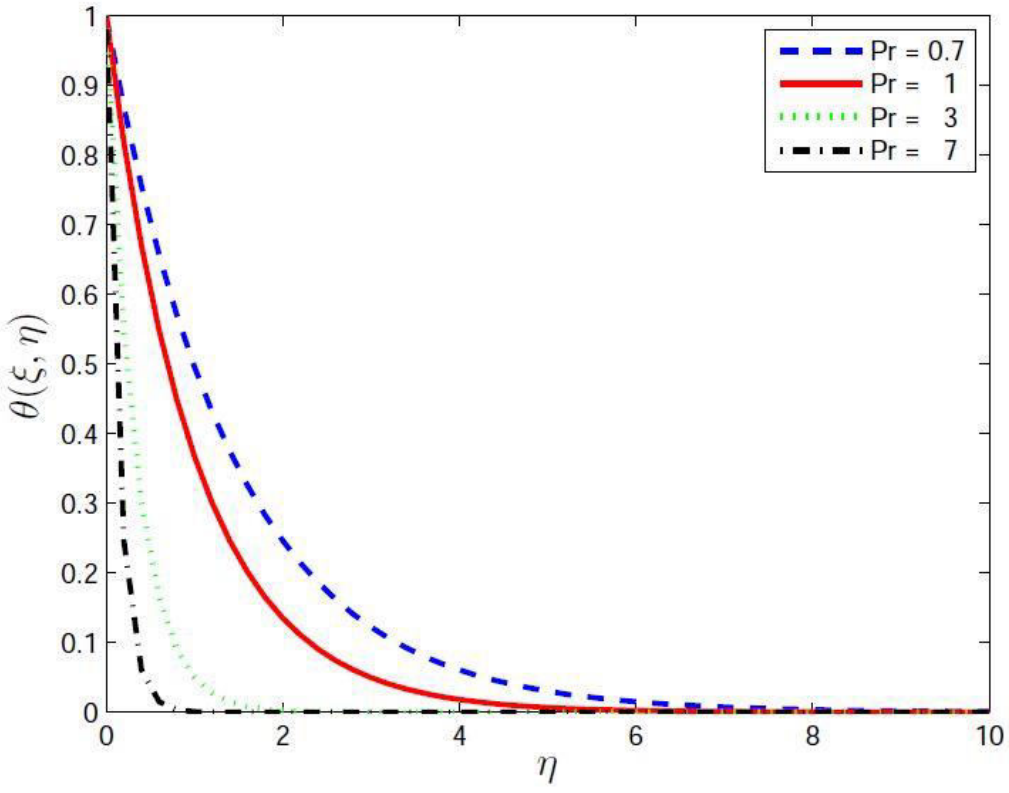

Figure-9. Temperature profile $\theta(\eta,\xi)$ for different values of Prandtl number Pr when $Pm = 0.7,\quad \xi = 2,$ and $S = 0.2$.

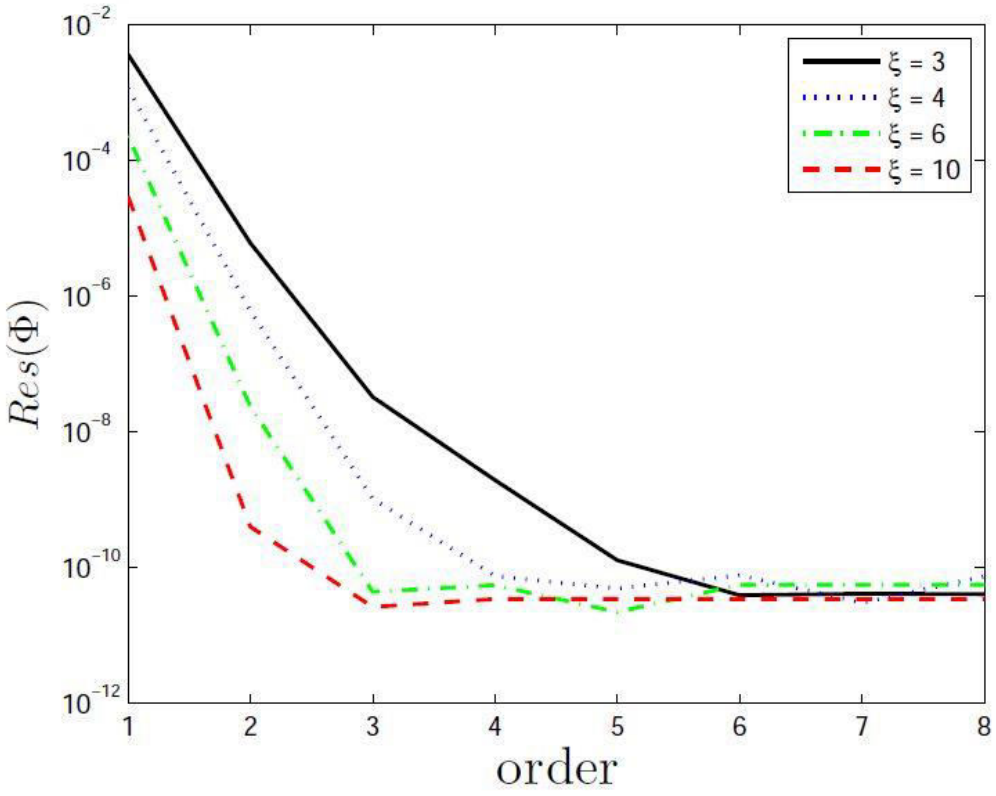

Figure-10. LSPM residual error curves $Res(F)$ for different values of ξ when $Pr = 0.7, S = 0.2, Pm = 0.7, L = 50,$ and$N_x = 100$.

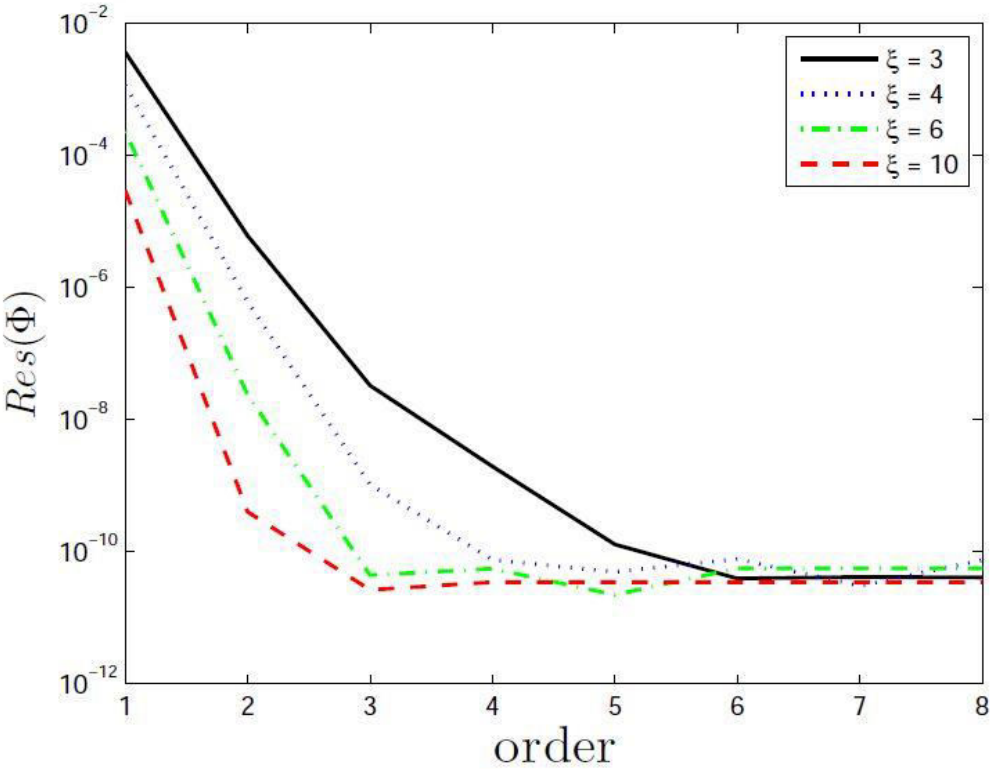

Figure-11. LSPM residual error curves $Res(\Phi)$ for different values of ξ when $Pr = 0.7, S = 0.2,$ and $Pm = 0.7\ L = 50, N_x = 100$.

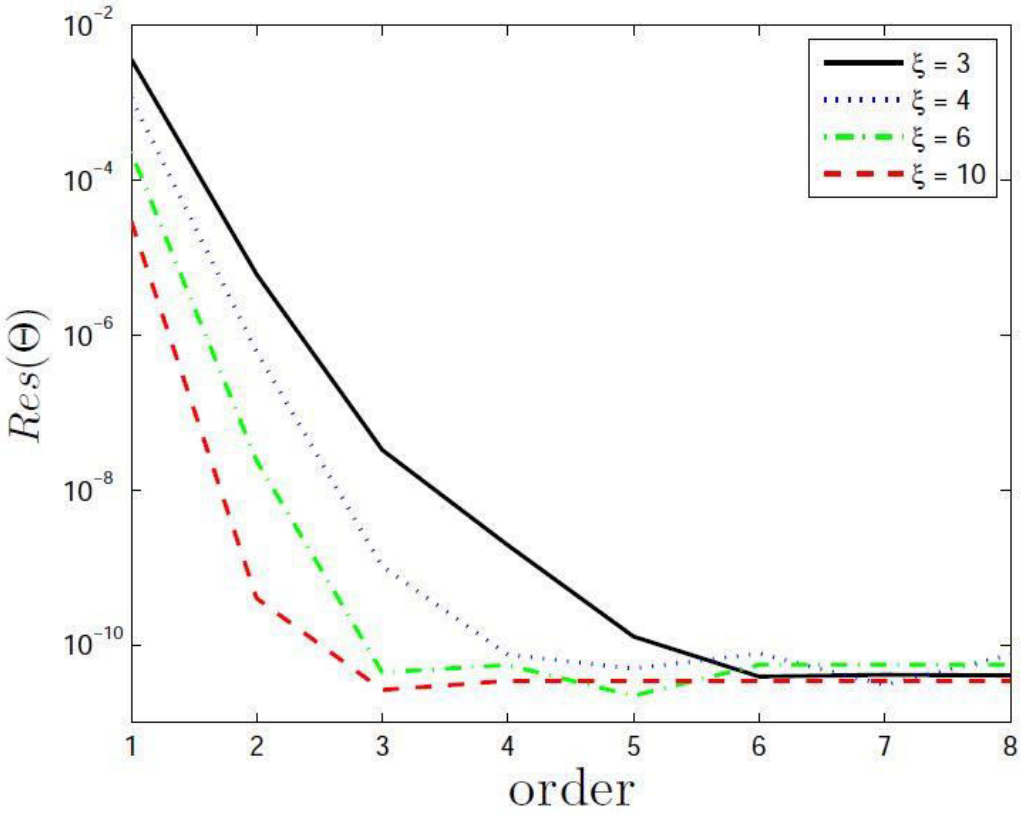

Figure-12. LSPM residual error curves $Res(\Theta)$ for different values of ξ when $Pr = 0.7, S = 0.2, Pm = 0.7, L = 50,$ and $N_x = 100$.